NASA Technical Memorandum 4089

Flight Tests of Three-Dimensional Path-Redefinition Algorithms for Transition From Radio Navigation to Microwave Landing System Navigation When Flying an Aircraft on Autopilot

Richard M. Hueschen
Langley Research Center
Hampton, Virginia

National Aeronautics
and Space Administration

**Scientific and Technical
Information Division**

1989

Summary

This report contains results of flight tests for three path-update algorithms designed to provide a smooth transition for an aircraft guidance system from measurements from distance measuring equipment and very-high-frequency omnirange stations and barometric navigation aids to the more precise Microwave Landing System (MLS) by modifying the desired three-dimensional flight path. The first algorithm, call zero crosstrack, eliminates the discontinuity in crosstrack and altitude error at transition by designating the first valid MLS aircraft position as the desired first way point while retaining all subsequent way points. The discontinuity in track angle is left unaltered. The second, called tangent path, also eliminates the discontinuity in crosstrack and altitude errors and chooses a new desired heading to be tangent to the next oncoming circular-arc turn. The third, called continued track, eliminates the discontinuity in crosstrack, altitude, and track-angle errors by accepting the current MLS position and track angle as the desired ones and recomputes the location of the next way point. The flight tests were conducted on the Transportation Systems Research Vehicle (TSRV), a small, twin-jet transport aircraft modified for research, under the Advanced Transport Operating Systems (ATOPS) program at the Langley Research Center. The flight tests showed that the algorithms provided a smooth transition to the MLS.

Introduction

The development of the Microwave Landing System (MLS) and its implementation at airports will expand the coverage and precision of aircraft-position data for the approach-through-landing phase of flight over that being provided presently by the Instrument Landing System (ILS). The ILS signal coverage is typically $\pm 2.5^\circ$ about the runway centerline and $\pm 0.7^\circ$ about a fixed glide slope (approximately a 3° slope). An MLS installation can provide volumetric coverage up to $\pm 60^\circ$ in azimuth about the runway centerline, 1° to 20° in elevation from the glide-path intercept point, and range coverage up to 20 n.mi. within the angular coverage. Thus, the expanded coverage will provide precise position data in areas where only less-precise radio navigation (RNAV) was available in the past. The use of the MLS data in the expanded coverage area will allow more flexibility and precision in air traffic control, and this, in turn, should result in increased terminal-area capacity.

A situation normally encountered when flying into MLS data coverage is depicted in figure 1. In this figure, the aircraft has just entered the MLS coverage (the shaded area) and the autopilot is controlling the aircraft on the three-dimensional (3D) desired path (the path stored in the flight control computer) using the RNAV-estimated aircraft position. However, the MLS-estimated aircraft position, which is the more accurate estimate, shows the aircraft position to be to the right of the desired path (it could be offset in other directions as well as having large altitude differences). If there were a simple switch to the MLS-estimated aircraft position, large guidance errors, e.g., crosstrack and altitude errors, would immediately be seen by the 3D autopilot control system. As a result, large, abrupt, pitch and roll maneuvers would be initiated as the autopilot nulled these guidance errors. Such maneuvers could be disconcerting to the passengers. Thus, algorithms to eliminate or reduce the magnitude of these autopilot maneuvers are desirable.

Under the Advanced Transport Operating Systems (ATOPS) program at the Langley Research Center, research efforts were performed to develop and flight test techniques for a smooth transition to the MLS under 3D (horizontal- and vertical-path tracking) autopilot operation. The approach used to provide the smooth transition was to develop algorithms that redefine the 3D desired path such that the guidance errors are small or zero at the time that the switch to MLS navigation is made. As a result, the autopilot "sees" small guidance errors when the switch to MLS navigation occurs, which precludes sudden aircraft maneuvering (particularly the type that might be perceived by passengers as being unusual). Although other approaches could have been used to reduce autopilot maneuvers (e.g., control law modification or some sort of path-recapture logic), the path-redefinition approach appeared to be the simplest and most desirable solution to the problem. This research resulted in three path-redefinition algorithms—called zero crosstrack (ZCT), tangent path (TP), and continued track (CT) (refs. 1, 2, and 3).

These algorithms were designed for installation in the flight control computers of the Transportation Systems Research Vehicle (TSRV)—a small, twin-jet, transport research aircraft (a Boeing 737) operated by the ATOPS office. The algorithms were developed to work within the 3D desired path structure of the TSRV fly-by-wire flight control system. The 3D desired path structure consists of straight lines (great-circle segments) and circular-arc segments specified by way points (a point defined by latitude, longitude, and altitude) and turn radii. From this path specification, lateral and vertical profiles are defined which the flight-control-system autopilot tracks.

The path-redefinition algorithms redefine a portion of the 3D desired path stored in the TSRV flight control computers which, for the remainder of this report, will be called simply "the desired path." The redefined path starts at the current MLS-estimated aircraft position and merges with the desired path in one of three ways depending on the algorithm being used. References 1, 2, and 3 describe the algorithms and associated equations and contain evaluation results obtained from nonlinear aircraft simulation runs which included sensor errors.

This report will present results of a flight test of the three algorithms. First, the three algorithms will be briefly described. Next, a description of the test configuration will follow. Then, the various tests conducted will be described followed by a discussion of the results. Finally, some concluding remarks will be given.

Acronyms and Symbols

Acronyms:

ATOPS	Advanced Transport Operating Systems
AZ	azimuth antenna
CRT	cathode-ray tube
CT	continued-track, 3D, path-redefinition algorithm
DME	distance-measuring equipment
3D	three-dimensional
EL	elevation antenna
ILS	Instrument Landing System
MLS	Microwave Landing System
NCDU	navigation control display unit
RNAV	radio navigation
R/W	runway
TP	tangent-path, 3D, path-redefinition algorithm
TSRV	Transport Systems Research Vehicle
ZCT	zero-crosstrack, 3D, path-redefinition algorithm

Symbols:

$Hdot$	vertical velocity, ft/sec
Δh	altitude error from desired vertical path, positive above, ft
Δy	crosstrack error (perpendicular position offset from desired lateral path), positive to right of path, ft
$\Delta\psi_{tk}$	track-angle error from desired lateral-path track angle, positive to right, deg

Description of Path-Update Algorithms

General Description

This section of the paper describes how the ZCT, TP, and CT algorithms redefine the desired path. Before the algorithms are defined, a brief description of the 3D guidance and control system will be given as an aid in understanding how the algorithms operate.

The 3D guidance and control system has two guidance and control laws—vertical- and horizontal-path laws (ref. 4). The vertical-path guidance and control law generates commands to the autopilot as a function of altitude, altitude rate, and vertical-acceleration guidance errors computed relative to the vertical profile of the desired path. The horizontal-path guidance and control law generates commands to the autopilot as a function of crosstrack (the perpendicular distance offset from path) and track-angle guidance errors computed relative to the horizontal profile of the desired path. The basic goal in the development of the path-redefinition algorithms was to update the path such that some or most of these guidance errors were zero at the time of transition to the MLS since small guidance errors result in small-magnitude autopilot maneuvers.

The major part of the development focused on techniques to redefine the horizontal profile of the desired path since the larger differences between the MLS- and RNAV-estimated aircraft positions are normally in the lateral estimates rather than in the vertical estimates. Thus, the names of the algorithms reflect the technique being used for the redefinition of the horizontal profile of the desired path. However, the vertical profile of the desired path is also redefined to minimize vertical maneuvers at transition, and its redefinition is a function of the lateral-profile redefinition. The redefinition of the vertical profile will be described under the "Vertical-Profile Redefinition" subsection.

Zero-Crosstrack (ZCT) Algorithm

The zero-crosstrack (ZCT) algorithm, which is the simplest of the three algorithms, was the first

to be developed and will be described with the aid of figure 2. As the name implies, the ZCT algorithm redefines the horizontal profile such that the crosstrack guidance error (Δy) is zero when the MLS navigation is selected. Figure 2 shows the horizontal desired profile (the heavy solid line) stored in the flight computer, the redefined ZCT profile (the lighter crosshatched line), the RNAV-estimated aircraft position, and the MLS-estimated aircraft position. When the aircraft enters MLS coverage, the ZCT algorithm defines new path segments that form a path from the MLS-estimated aircraft position back to the desired path. The first straight-line segment falls on a line between the MLS-estimated aircraft position and point P, that is, the intersection of the current and next straight-line segments of the desired path. Next, a redefined circular arc, having the same radius as the desired path turn, is fit by the ZCT algorithm into the corner of the new and next straight-line segments. This redefinition ensures that the aircraft will be on the redefined path when the redefined path and the MLS navigation mode are selected. A characteristic of this algorithm is that it typically creates a track-angle guidance error ($\Delta\psi_{tk}$) at the transition to the MLS as is shown in figure 2. In fact, this error will only be zero when the aircraft ground track lies in the same direction as the new straight-line segment, which is not likely. Thus, some aircraft maneuvering will usually result for this algorithm at transition as the autopilot responds to the nonzero track-angle error even though the crosstrack error is zero.

A potentially undesirable aspect of this algorithm is that the turn-segment part of the redefined path is moved from the original desired turn segment. If this turn is the one onto the runway centerline, the intersect point of the redefined path on the runway centerline, point C1 of figure 2, can be shifted closer or farther from the runway (e.g., a mile or more), and this might not be desirable in certain air traffic control situations (e.g., noise-restricted areas on the ground or violations of the aircraft-spacing requirements). The direction that the turn moves depends on the MLS-estimated aircraft position relative to the desired path. For example, if the MLS aircraft position were to the left instead of to the right of the desired path in figure 2, the redefined turn would have been to the left of the desired turn.

Tangent-Path (TP) Algorithm

The tangent-path (TP) algorithm was developed to prevent the movement of the redefined turn. As the name implies, the TP algorithm redefines the desired path by forming a straight-line segment from the MLS-estimated aircraft position to the point of tangency on the next desired turn segment. Like the ZCT algorithm, the crosstrack error is zero when the switch to the redefined path and MLS navigation occurs. Figure 3 shows two cases for the MLS-estimated aircraft position. If the MLS aircraft position is to the right of the desired path (case 1), the point of tangency will be at B1 in figure 3. If the MLS aircraft position is to the left of the desired path (case 2), the point of tangency, point B2, will be on a circular extension of the desired path. In either case, the desired turn segment does not move, although the turn angle will change as a function of the MLS aircraft position. A disadvantage of this algorithm compared with the ZCT algorithm is that its track-angle error at transition can be large, particularly when the aircraft is close to the start of the original desired turn and has a large lateral displacement from it. Thus, this algorithm may result in more maneuvering at transition than the ZCT algorithm, but it does not cause the desired turn segment to be moved.

Continued-Track (CT) Algorithm

The continued-track (CT) algorithm was developed to eliminate the track-angle error that exists at transition for both the TP and ZCT algorithms. The CT algorithm redefines the desired path by specifying a straight-line segment that begins at the MLS-estimated aircraft position and extends along the direction of the instantaneous estimated MLS direction of flight as shown in figure 4. The straight line is projected to the intercept point on the next straight-line segment, point P; and a circular-arc segment, with the same radius as the original desired path turn, is placed into the corner of the straight-line segments. Thus, as shown in figure 4, the turn segment can be displaced considerably away from the original desired turn segment (particularly if the flight direction were away from the original desired path). As a result of this path redefinition, both the crosstrack and the track-angle lateral guidance errors are zero at transition to the MLS; therefore, no aircraft lateral maneuvering occurs at transition. Normally, the MLS-estimated direction of flight would be approximately parallel to the straight-line segment of the desired path. However, to illustrate the operation of the CT algorithm, the direction of flight was shown somewhat different which, in reality, can happen in the presence of wind upsets.

The CT algorithm also has the ability to redefine the path while the autopilot is tracking a turn segment when the switch to MLS navigation occurs. (The ZCT and TP algorithms do not have this feature.) When on a circular-path segment, the CT algorithm builds a redefined path as illustrated in figure 5. It builds a circular-arc segment, with the

same radius as the current desired turn, starting at the MLS aircraft position. The algorithm extends the new circular arc to a point where a straight-line segment is tangent to both this arc, point C1, and the next circular-arc segment of the desired path, point D1. If the transition to the MLS occurs on the last turn onto the runway centerline, the CT algorithm builds a circular-arc segment from the MLS aircraft position to a tangency point on runway centerline. The algorithm achieves this by changing the radius of the current desired turn. In some cases, the resulting radius of turn may be too small for the aircraft to follow, or the MLS-estimated aircraft position may even be on the other side of the runway centerline because of a large error in the RNAV-estimated aircraft position. Algorithms and logic have not yet been developed to cope with these cases. However, for operational applications, these cases will have to be taken into account even though they do not usually occur because the transition to the MLS will have occurred at a sufficiently earlier point in time prior to reaching the final turn segment.

Comparison of Algorithms

By design, the CT algorithm is the best of the three algorithms in terms of minimizing transition maneuvering. However, it and the ZCT algorithm move the next turn segment when the transition to the MLS occurs on a straight-line segment. Generally, the turn segment is moved more by the CT algorithm than by the ZCT algorithm. (Compare figs. 2 and 4.) The TP algorithm is best in this regard since it not only does not move the next turn segment but also it generally is the worst in terms of transition maneuvering. However, this maneuvering may be acceptable in cases where the next turn segment cannot be moved because of aircraft control restrictions. Another advantage of the CT algorithm is that only it redefines the path when MLS transition occurs on a turn segment. Thus, the CT algorithm provides more time flexibility for the transition to the redefined path and for when MLS navigation can occur. The ZCT and TP algorithms are further restricted because they cannot be practically used when track-angle error is large at transition to MLS navigation. Large track-angle errors can cause autopilot maneuvers that are large enough to alarm passengers. (For example, large track-angle errors will occur when the aircraft is close to the turn segment (i.e., less than 5000 ft) and has a large crosstrack error (i.e., greater than 3000 ft) relative to the original desired path.)

Vertical-Profile Redefinition

The desired vertical profile of the desired path is a series of straight lines that are connected at the various way points of the desired path as shown by the solid line in figure 6. Each straight line has a fixed glide slope that is calculated from the altitude difference and the distance between the way points at the ends of each straight line.

The vertical-profile redefinition for each algorithm consists of redefining the altitudes for the redefined way points that were computed during the lateral-profile redefinition. For each of the algorithms, the desired altitude of the beginning of the redefined path is set equal to the MLS-estimated aircraft altitude; this is where the redefined path begins that will result in a zero-altitude error (Δh) at transition. The altitude-profile redefinition for the remainder of the redefined path varies with each algorithm.

For the ZCT algorithm, the desired altitude profile is determined by first computing the desired altitude at the end of the redefined turn. This altitude is computed so that the glide slope after the redefined turn (after point C1 of fig. 6) is the same as the glide slope after the original desired turn (glide slope after point C). Next, the desired altitude at the start of the redefined turn is established. (See point B1 of fig. 6.) This altitude is defined such that a constant glide slope results between the MLS-estimated aircraft position and the end of the redefined turn. The constant glide slope is computed by dividing the distance from the aircraft to the end of the redefined turn into the altitude difference between the MLS-estimated aircraft altitude and the desired altitude at the end of the redefined turn. Finally, the desired altitude at the start of the turn is set to lie on the computed glide slope.

For the TP algorithm, the altitude at the end of the redefined turn remains the same as that for the desired turn. The altitude of the redefined start of the turn (i.e., points B1 or B2 in fig. 3) was intended to be defined in the same way as for the ZCT algorithm (namely, set to lie on a constant glide slope between the MLS aircraft position and the end of the turn); however, the implementation was slightly different. In the implementation, the altitude at the redefined start of the turn was set equal to the altitude at the start of the original desired turn (point B in fig. 3). Therefore, the difference from the ZCT algorithm is that the glide slope on the turn will generally not be the same as the glide slope approaching the turn.

For the CT algorithm, the altitude redefinition is the same as that for the ZCT algorithm when the transition to the MLS is made along a straight-line segment. When in a turn, the altitude of the start of the redefined turn is set to the MLS-estimated altitude. The remaining profile-altitude redefinition is dependent on whether the redefined turn is the final turn to the runway. If on the final turn, the

altitude at the end of the redefined turn is set so that the glide slope to the runway remains the same as the original desired glide slope. If not on the final turn, the altitude at the end of the turn is set to maintain a constant glide slope from the current MLS position to the start of the next turn. If any way points are between the turns, their altitudes are set to lie on that glide slope.

Description of Test Setup

The three algorithms were tested on the ATOPS TSRV aircraft (a Boeing 737) shown is figure 7. The aircraft is equipped with an aft research cockpit mounted inside the cabin just forward of the wing. This cockpit is outfitted with cathode-ray-tube (CRT) displays and a navigation control display unit (NCDU). The NCDU allows the pilot to enter data into the navigation and guidance computers and has a small CRT to confirm his entries and to display information to the pilot. One CRT, called a navigation display, shows the desired 3D flight path with the estimated aircraft position shown relative to this path. The TSRV is also equipped with magnetic recorders used to store the desired flight test data. In addition to a standard set of recorded variables, selected data such as crosstrack, track-angle, and altitude errors and data for estimated RNAV and MLS aircraft positions were recorded.

The equations for the algorithms were installed as software in the navigation computer. Software was also installed to display the redefined path to the pilot when the MLS became valid and to define two buttons on the NCDU to allow him to accept or reject the redefined path. One button was defined the "accept" button. If the pilot pushed it, the redefined path and MLS navigation were selected. The other button was defined as the "reject" button. When the pilot pushed it, MLS navigation was selected, but the redefined path was rejected and thus the original desired path remained; this normally resulted in large autopilot maneuvers. Thus, pushing the "reject" button represented the condition where the 3D autopilot nulls the guidance errors without redefining the path. If the pilot does not push either button, the 3D autopilot would continue to use the RNAV-estimated aircraft position and the original desired path; during this time the redefined path, computed from the MLS-estimated aircraft position, would be continuously updated on the display. For the tests presented, the pilot always pushed one of the buttons.

The baseline set of guidance and control laws for the TSRV were in place for the tests (documentation on the laws is available upon request from the Boeing Commercial Aircraft Company in-house documentation). The 3D flight control mode, which consists of horizontal- and vertical-path guidance and control laws (ref. 4), was used for the tests and was briefly described earlier. The airspeed hold mode was also used so that airspeed and path control were entirely automatic for these tests. The baseline control laws use measurements from the air data computers, aircraft sensors, and inertial platforms to provide relatively precise navigation, guidance, and control compared with that of current commercial airline operation.

The tests were conducted at the NASA Wallops Flight Facility using two 3D approach paths to runway 22. The two approach paths, STAR WFB13 and STAR WFSBB, are shown, respectively, in figures 8 and 9. WFB13 contains one 130° turn just before the turn onto the runway centerline, and WFSBB contains two 90° turns just prior to the runway centerline. These paths are stored in the navigation computer by way point specification (latitude, longitude, altitude, desired airspeed, and associated turn radii). The desired altitude, desired airspeed, and names of the way points are shown in the figures.

The MLS installation at Wallops is located on runway 22 and has azimuth, elevation, and DME antennas to provide 3D MLS navigation. The azimuth and range antennas provide signals $\pm 60°$ about runway centerline, and the elevation antenna provides signals from 1° to 20° in elevation in the same azimuth region.

Description of Tests

Eleven test runs were conducted for this flight test—eight on flight path WFB13 and three on flight path WFSBB. Each test run was designed to test a preselected algorithm. There was no attempt to select the "best" algorithm for the situation that existed at the transition to MLS navigation. Rather, in most cases, the tests were designed to set up nearly equal initial conditions for each algorithm so that they could be compared with each other.

Prior to starting each test run, the test pilot maneuvered the aircraft to enter the selected 3D path (WFB13 or WFSBB) at the beginning way point with the specified altitude and airspeed. Then, the pilot armed the 3D control system for automatic engagement. (This normally occurred simultaneously because the pilot had steered the aircraft close enough to the 3D path to satisfy engage conditions.) He also engaged the airspeed hold mode if not done earlier. When the 3D control system and airspeed hold were engaged, the test run was ready to begin.

For flight path WFB13, the test run began in the turn between way points WFBBB and WFBBC (fig. 8). For flight path WFSBB, the test run began in the turn between way points WSBBB and WSBBC

(fig. 9). In order to simulate the less-precise navigation of current airline operations, a position bias was inserted into the RNAV solution prior to entering MLS coverage and navigation position measurements were inhibited. When the RNAV-estimated aircraft position crossed WFBBC for path WFB13 and WSBBC for path WFSBB, the position bias was inserted into the RNAV solution. This position bias was used to define the RNAV-estimated aircraft position laterally away from the desired path so that a large difference would exist, between the RNAV- and MLS-estimated aircraft positions, when the switch to MLS navigation occurred. (See fig. 10.) Two types of biases were used in the tests: (1) a bias that resulted in the MLS-estimated position being located to the right of the desired path when the switch to MLS navigation occurred, and (2) a bias that resulted in the MLS position to the left of the desired path. To make the MLS-estimated aircraft position be to the right of the desired path, a position bias was inserted into the RNAV solution to make the RNAV-estimated aircraft position be initially left of the desired path. In response to the crosstrack error created by the inserted bias (fig. 10), the control system maneuvered the aircraft to the right to null the crosstrack error. This maneuvering results in the MLS-estimated aircraft position which is to the right of the desired path. The opposite procedure was followed to make the MLS aircraft position fall to the left of the desired path at transition.

When the MLS became valid, the redefined path was shown on the navigation display along with the existing desired path for the pilot and test personnel to observe. Figure 11 illustrates a typical display of information on the navigation display immediately after the MLS became valid. After observing the navigation display for a short time, the pilot either rejected or accepted the redefined path by pushing the appropriate button according to the flight test plan. If the path was rejected, the redefined-path segments were removed from the map display, and the autopilot maneuvered the aircraft back to the desired path using MLS-estimated aircraft position and velocity. If the path was accepted, only the redefined path was left of the navigation display, and the 3D autopilot tracked the redefined path using MLS estimates. Note that for both rejection and acceptance of the redefined path, the control system was switched to MLS navigation. The main interest of the test runs was to observe and record the aircraft maneuvers from the time that the switch to MLS navigation occurred to the time when the aircraft completed the turn onto the runway centerline. When the aircraft reached the runway centerline, the test run was completed.

A summary of the test runs is compiled in table I. It lists the flight path used for the test run, the position-bias offset inserted into the RNAV solution, and the path-redefinition algorithm used for the test run. Note that for runs 1 and 2 the redefined path was rejected (in accordance with the flight test plan). For the remainder of the runs, the redefined path and the MLS solution were used.

Table I. Summary of Test Runs

Test run	Flight path	Inserted position offset (a)	Path-redefinition algorithm	Comments
1	WFB13	1560 ft right	ZCT	Reject redefined path as per test plan
2	WFB13	3220 ft right	ZCT	Reject redefined path as per test plan
3	WFB13	3220 ft right	ZCT	
4	WFB13	3250 ft left	CT	Logic switched to CT from ZCT (too close to turn)
5	WFB13	3280 ft left	ZCT	
6	WFB13	3200 ft right	TP	
7	WFB13	3200 ft right	CT	
8	WFB13	3200 ft left	CT	Redefine path during turn
9	WFSBB	4000 ft left	CT	Logic switched to CT from ZCT (MLS engaged during turn)
10	WFSBB	2000 ft left	CT	
11	WFSBB	2000 ft left	CT	Redefine path shortly after coming out of large radius turn prior to two 90° turns

[a] "Right" denotes that MLS aircraft estimate appears to right of RNAV estimate.

Discussion of Test Results

Table II gives a summary of the test run results. The table has values for the crosstrack error (Δy), track-angle error ($\Delta\psi_{tk}$), altitude error (Δh) at the instant when the switch to MLS navigation occurs, and the maximum aircraft roll angle following the switch to the MLS. For the crosstrack errors, two values are given for each run (if available from recorded data): one for the error relative to the original desired path and the other relative to the redefined or new path.

Table II shows that the crosstrack errors relative to the original desired path for runs 1 and 2 at the switch to MLS navigation were, respectively, 759 ft and 8227 ft and the altitude errors were, respectively, −44 ft and −90 ft. The track-angle errors were both small since the redefined path was rejected (in accordance with the flight test plan) and because the desired ground track angle after the switch to MLS navigation is the same as that before the switch. This is to be expected because, although there is an offset between the RNAV and MLS desired path-position estimates, the straight-line segments of these paths are parallel.

Time history plots of selected parameters for test run 2 are shown in figure 12. As indicated in table I, the redefined path was rejected for this test run to illustrate the type of autopilot maneuvering that can occur without the path-redefinition capability. The parameters shown in figure 12(a) are crosstrack error (Δy), track-angle error ($\Delta\psi_{tk}$), and the aircraft roll attitude. Those in figure 12(b) are altitude error (Δh), the vertical velocity (*Hdot*), and the aircraft pitch attitude. As shown in figure 12(a), the insertion of the lateral-position offset occurred at 5 sec. The inserted offset caused the RNAV-estimated aircraft position to move to the left of the desired path which resulted in a negative crosstrack error (negative Δy). Thus, the autopilot rolled the aircraft to the right (positive roll) to null Δy. (Fig. 10 illustrates this situation.)

At slightly less than 135 sec the switch to MLS navigation occurred, as is shown by the sudden jump in Δy to 8227 ft. in figure 12(a). (Note that the 8227 ft is the MLS solution relative to the desired path and that at the position-bias insertion point, the RNAV solution most likely differed considerably from the true aircraft position when the 3220-ft bias offset was inserted. When valid, the MLS-estimated aircraft position is close to the true position.) The autopilot immediately rolled the aircraft left to −25° (maximum allowed by the autopilot) to null the positive crosstrack error, with the resultant negative track-angle error occurring as the crosstrack error was reduced. At 145 sec the autopilot reduced the roll attitude because the intercept angle (track angle relative to the desired track) was approaching the maximum value which is limited to 30° by the 3D guidance. At 180 sec the aircraft reached the final turn to the runway (point WFBBF in fig. 7) while still in the process of reducing the crosstrack error. At this point the guidance system automatically commanded a nominal roll attitude for the turn, and this resulted in the aircraft roll attitude of approximately −10° as shown in the plot. However, since the intercept angle was still at its maximum allowed value, the autopilot rolled the aircraft back to wings level or zero roll attitude. Then, as the crosstrack and track-angle errors were reduced toward zero values, the autopilot rolled the aircraft negatively to remain on the circular-path segment.

Table II. Summary Test Data at Point of Selecting MLS Navigation

Test run	Δy, ft, relative to— Original desired path	Δy, ft, relative to— New path	$\Delta\psi_{tk}$, deg, relative to new path	Δh, ft, relative to new path	Maximum roll after MLS engaged, deg
1	759	(a)	−1.4	−44	−11
2	8227	(a)	1.2	−90	−25 (Max allowed)
3	1945	8	3	−4.5	−5
4	−5304	−19	0	−20	2.5
5	−4887	−45	−10	−19	16
6	2570	71	8	0	−14
7	3368	−6	0	−7	No maneuvering
8	1990	0	0	−12	Update in turn
9	−3439	16	3	−17	Update in turn
10	−1818	0	0	−5	No maneuvering
11	2186	5	0	−9	No maneuvering

[a]Not applicable.

The data plot terminates at approximately the middle of the turn to the runway. Data were collected until the aircraft rolled out of the turn onto the runway centerline to check the 3D guidance to this point. However, the events in the transition to the MLS were completed at the point where the plot is terminated. As noted earlier, the roll maneuvering between wings level and the various roll attitudes described above could be alarming to airline passengers and operationally unacceptable to the pilot and air traffic control. The desire to reduce this maneuvering was the motivation for developing the path-redefinition algorithms.

Figure 12(b) shows that the switch to the MLS caused transients in pitch attitude and vertical velocity of 4° and 20 ft/sec (1200 ft/min), respectively. Again, these transient maneuvers could be alarming to the passenger, and the redefinition algorithms are intended to reduce these as well as the lateral maneuvers.

Time history plots of parameters for flight test run 3 are shown in figure 13. The position bias was inserted at approximately 15 sec, and at 150 sec the pilot selected the redefined path (the ZCT path-redefinition algorithm) at a point in the flight path similar to the aircraft position shown in figure 1. As a note, the plotted error parameters are determined in the flight computer from MLS navigation data when the switch to the MLS occurs. Thus, when the switch to MLS navigation occurs (at 150 sec in fig. 13), Δy, $\Delta\psi_{tk}$, and Δh are computed from MLS estimates relative to the desired path position as determined by the MLS. The crosstrack error at the switch to MLS navigation was 8 ft (see table II) and the track-angle error $\Delta\psi_{tk}$ was 3°. (See fig. 2 to understand why the track-angle error was positive at the switch to MLS navigation with the use of the ZCT algorithm.) The autopilot maneuvered the aircraft some to reduce these errors. The roll angle was perturbed from wings level to about −5°, which was estimated to be only slightly discernible to passengers. However, in some cases, the track-angle error could be larger which would cause larger maneuvers (e.g., when the lateral difference between the RNAV and the MLS is larger and when the aircraft is closer to the turn). Thus, if the track-angle error is small, the results of this run indicate that the ZCT algorithm will reduce maneuvering to acceptable levels at the transition to the MLS. However, finding the minimum track-angle error for acceptable maneuvering was not part of this effort.

Figure 13(b) shows the aircraft vertical response for test run 3. A very small amount of vertical maneuvering occurred at MLS transition (at 150 sec) because of a −4.5-ft-altitude error. (Such maneuvering will probably not be noticeable to airline passengers.) Vertical maneuvering after 180 sec is due to coupling of the roll maneuvers into the autopilot vertical control. (See the roll data of fig. 13(a).) The altitude error was not zero because the path-redefinition algorithms are updated in the navigation computer at a slower rate than the computation rate for the 3D autopilot controls. The redefined path is computed at approximately 1-sec intervals, whereas the control variables are updated 20 times per second. Thus, if the aircraft is descending or climbing and the switch to MLS navigation does not occur simultaneously with the desired altitude for the redefined path, an altitude error will result. It will be largest if the switch occurs just before a new desired altitude is computed. For example, if the aircraft is descending at 30 ft/sec, the altitude error at the switch could approach 30 ft.

The aircraft lateral and vertical responses for transition to the redefined path using the TP algorithm (test run 6) are shown, respectively, in figures 14(a) and 14(b). A 3200-ft, right-lateral position bias (one to make the MLS-estimated aircraft position appear to the right of the desired path at the switch to MLS navigation) was inserted at 15 sec as shown in figure 14(a). At 135 sec the switch to MLS navigation and the TP redefined path occurred which resulted in immediate errors in crosstrack, track angle, and altitude, respectively, of 71 ft, 8°, and 0 ft. The crosstrack error is supposed to be zero. However, the slower computation of the redefined path, as explained earlier, probably caused it to be nonzero. (See fig. 3 to note that the aircraft will be moving away from the TP redefined path between its updates.) These conditions resulted in a lateral maneuver lasting 30 sec with a maximum negative roll of 14° as shown in figure 14(a). The position conditions at the switch to MLS navigation were nearly the same for this test as for the ZCT algorithm test of figure 13(a). For the TP algorithm test, the aircraft was a little farther from the start of the turn to the runway which should reduce the maneuvering for the TP algorithm since the track-angle error at transition gets smaller as the aircraft is farther from the turn. Comparing this response with that of the ZCT path update of figure 13(a) shows that the TP algorithm results in more maneuvering than the ZCT algorithm. However, as noted in an earlier section of the report, the TP algorithm may be desirable in some air traffic control situations since it does not displace the final turn onto the runway centerline.

Figure 14(b) shows that the aircraft pitched up some at the transition to the updated path at 135 sec even though the altitude error was zero. The data are not conclusive as to why the aircraft pitched up, but

a possible reason is that the redefined path required a reduced descent angle. (The desired flight path angle was not recorded.) The plot of vertical velocity (*Hdot*) shows that the average rate of descent is reduced after the transition. The overall result of the run is that the vertical response is small, and most likely passengers will not recognize this response over that of other vertical aircraft responses on a typical normal flight.

The aircraft response at the switch to MLS navigation for a CT redefined path along a straight-line segment is shown in figure 15 (test run 7). The switch to MLS navigation and the CT redefined path occurred at 145 sec into the test run. The errors in crosstrack, track angle, and altitude at this time were, respectively, −6 ft, 0°, and −7 ft. The altitude error is nonzero because the aircraft has descended some since the redefined path was updated (path update at 1-sec intervals, minimum). As figure 15(a) shows, there is no lateral maneuvering at transition to the redefined path. Only a slight amount of vertical maneuvering occurs as shown in figure 15(b), and most of that may be caused by a wind-turbulence increase. (See the pitch and *Hdot* plots just prior to the transition.) This test run shows that the CT algorithm results in the least maneuvering at transition, but as discussed in the description of the algorithm, it results in the next turn segment being moved the most in the updated path. Of course, this may or may not be a problem depending on air traffic control considerations.

The aircraft response for transition to the redefined path and MLS navigation when in a turn (only the CT algorithm is capable of path redefinition in the turn) is shown in figure 16 (test run 8). The transition to the updated path occurred at approximately 200 sec just after the aircraft began rolling into the turn. As the figures show, the response to the transition is barely noticeable.

Test run 9 was conducted on flight path WFSBB, which is shown in figure 9. This run was intended to use the ZCT algorithm but, apparently, switch-contact problems (on the button to accept the redefined path and on the switch to MLS navigation) prevented the pilot from switching to MLS navigation and to the redefined path until in the next-to-last turn to the runway. Since the ZCT algorithm cannot update the path in a turn, the logic installed in the path update software defaulted the system to the CT algorithm. Thus, for this test run, the transition was made in the turn using the CT redefined path. The aircraft had a slight response to the transition, but this response will not be shown since it was similar to the response of run 8 shown in figure 16(a).

Both test runs 10 and 11 used the CT algorithm and flight path WFSBB. For run 10 the transition to the redefined path was made just prior to way point WSBBF. For run 11 the transition was just after way point WSBBC, with the bias offset for this run being inserted in the large turn just after way point WSBBB; this was a deviation from the general test plan for bias insertion. The aircraft response for both of these runs was essentially the same. That is, no lateral response and barely noticeable vertical response at transition. Thus, no data plots will be shown for these runs.

Concluding Remarks

Three path-redefinition algorithms for the transition to the Microwave Landing System (MLS) were flight tested, and they performed approximately as expected. That is, the tangent-path (TP) algorithm resulted in the most maneuvering at transition to the MLS and the continued-track (CT) algorithm resulted in the least. In fact, the CT algorithm resulted in essentially no lateral response at transition. However, it displaces the final turn the most, which could be unacceptable in certain air traffic control situations.

There was some vertical response of the aircraft for all algorithms at transition, but the response would, most likely, not be noticeable to the average airline passenger. Some of the lateral responses might be noticeable but probably would not be objectionable.

In summary, each of the algorithms reduce aircraft maneuvering at the transition to the MLS. However, further research is required to investigate the suitability of the algorithms for various path geometries and to develop logic to address air traffic control procedures before this approach to MLS transition would be recommended as a viable operational method.

References

1. Pines, Samuel: *Terminal Area Automatic Navigation, Guidance, and Control Research Using the Microwave Landing System (MLS). Part 2—RNAV/MLS Transition Problems for Aircraft.* NASA CR-3511, 1982.
2. Pines, Samuel: *Terminal Area Automatic Navigation, Guidance, and Control Research Using the Microwave Landing System (MLS). Part 3—A Comparison of Waypoint Guidance Algorithms for RNAV/MLS Transition.* NASA CR-3512, 1982.
3. Pines, Samuel: *Terminal Area Automatic Navigation, Guidance, and Control Research Using the Microwave Landing System (MLS). Part 4—Transition Path Reconstruction Along a Straight Line Path Containing a Glideslope Change Waypoint.* NASA CR-3574, 1982.
4. White, William F., compiler: *Flight Demonstrations of Curved, Descending Approaches and Automatic Landings Using Time Reference Scanning Beam Guidance.* NASA TM-78745, 1978.

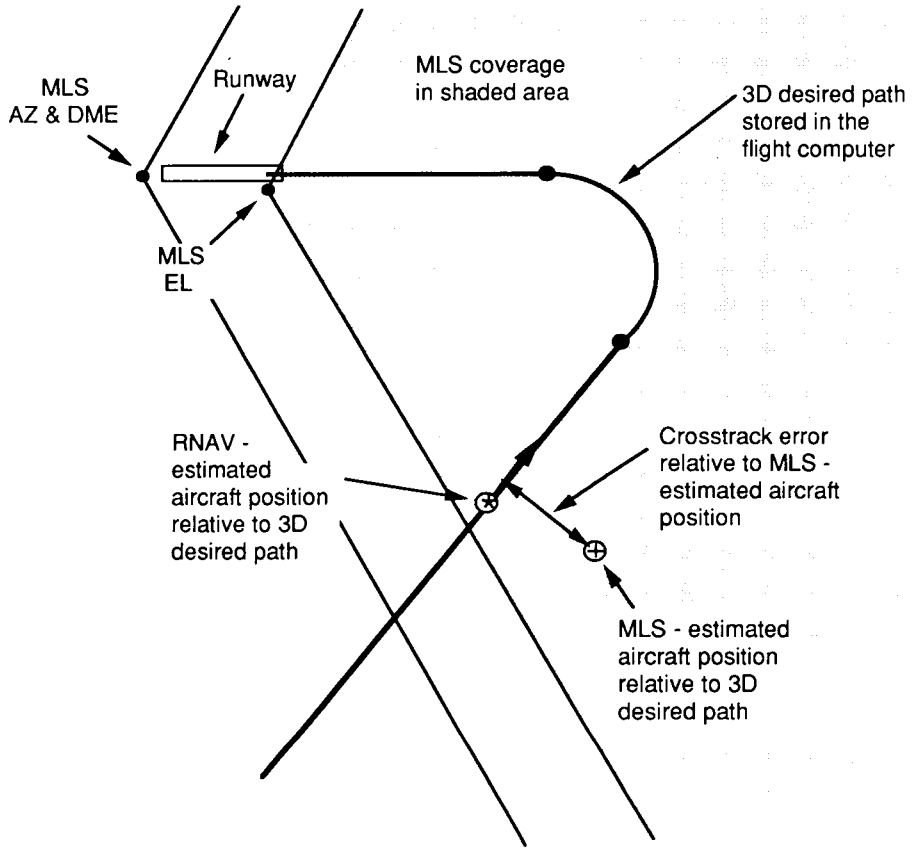

Figure 1. RNAV and MLS estimates of aircraft position relative to desired path.

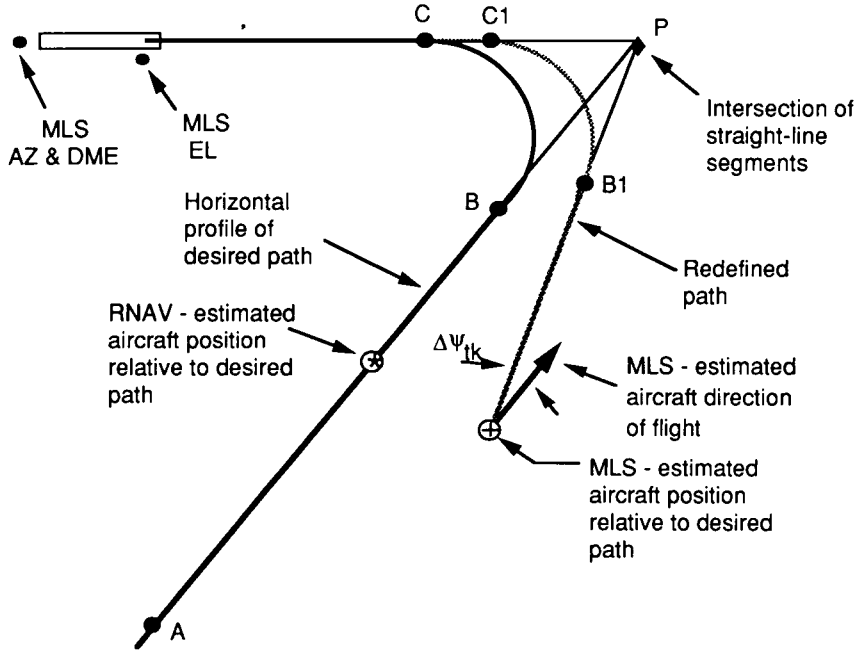

Figure 2. Path redefinition with zero-crosstrack (ZCT) algorithm.

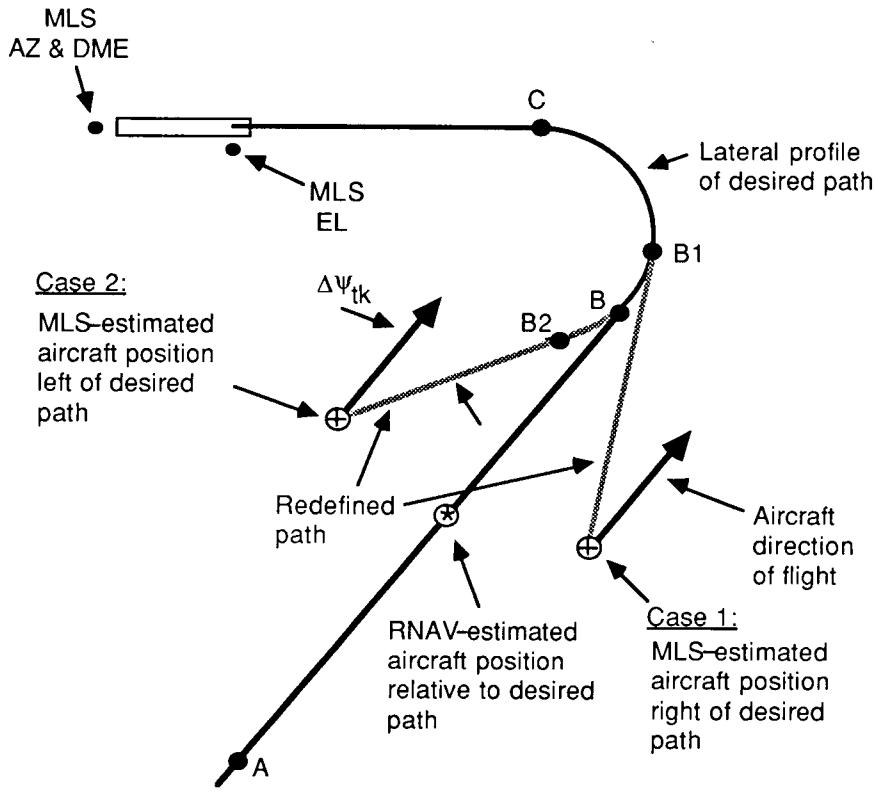

Figure 3. Path redefinition with tangent-path (TP) algorithm.

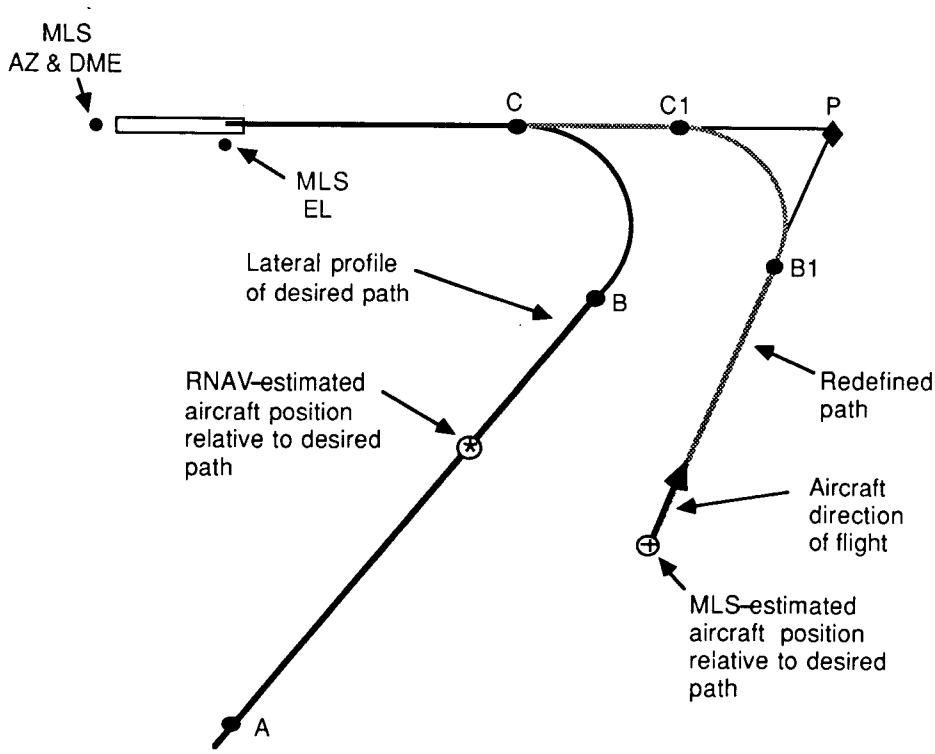

Figure 4. Path redefinition on straight line with continued-track (CT) algorithm.

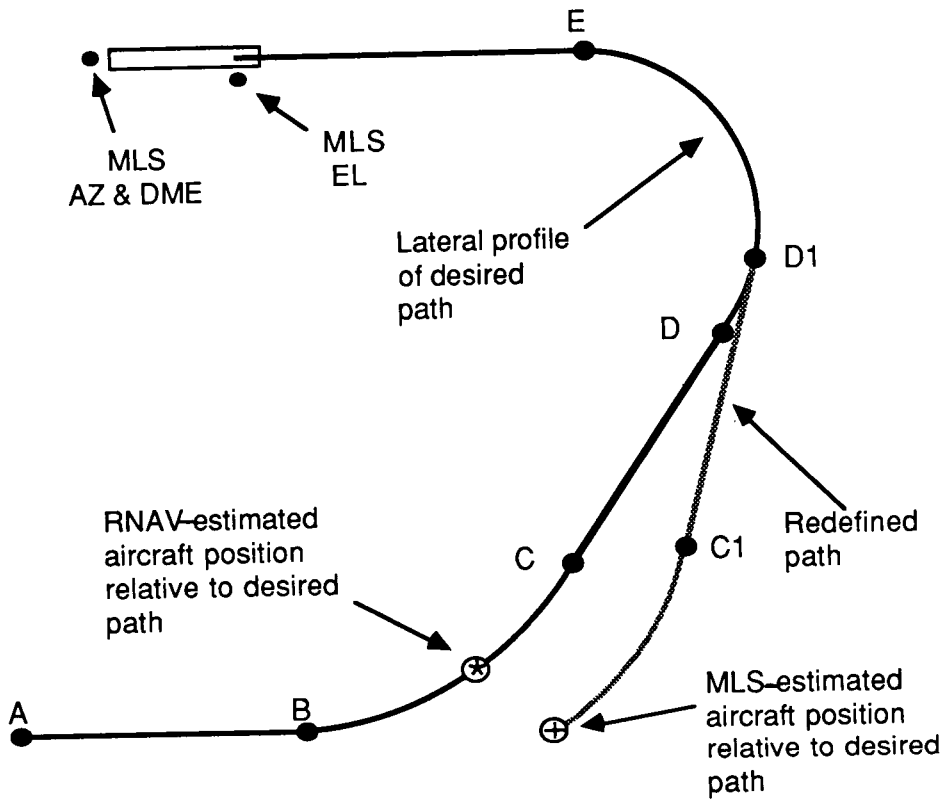

Figure 5. Path redefinition during turn with continued-track (CT) algorithm.

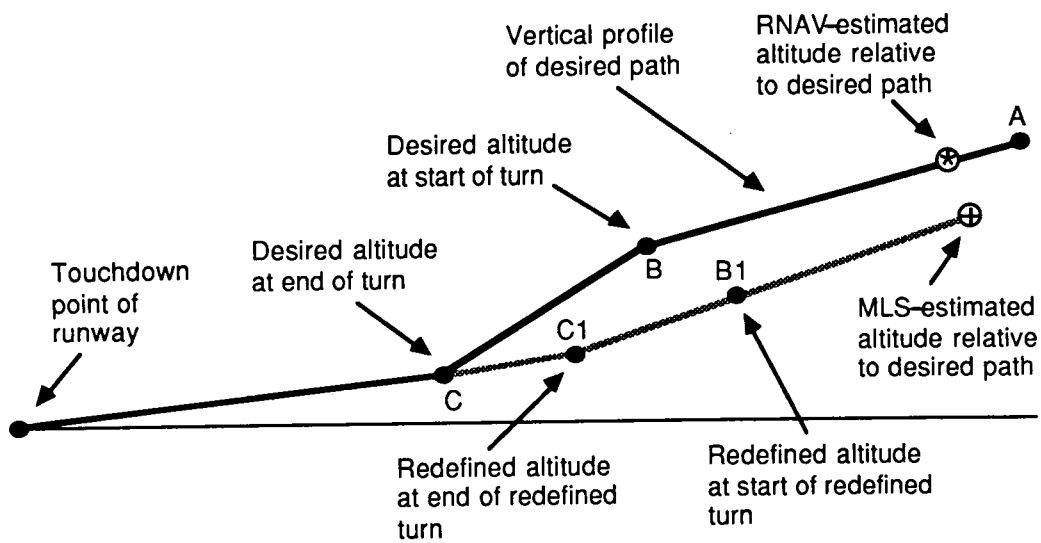

Figure 6. Vertical-profile redefinition for MLS transition on straight line.

L-73-6283

Figure 7. The ATOPS TSRV aircraft (a Boeing 737).

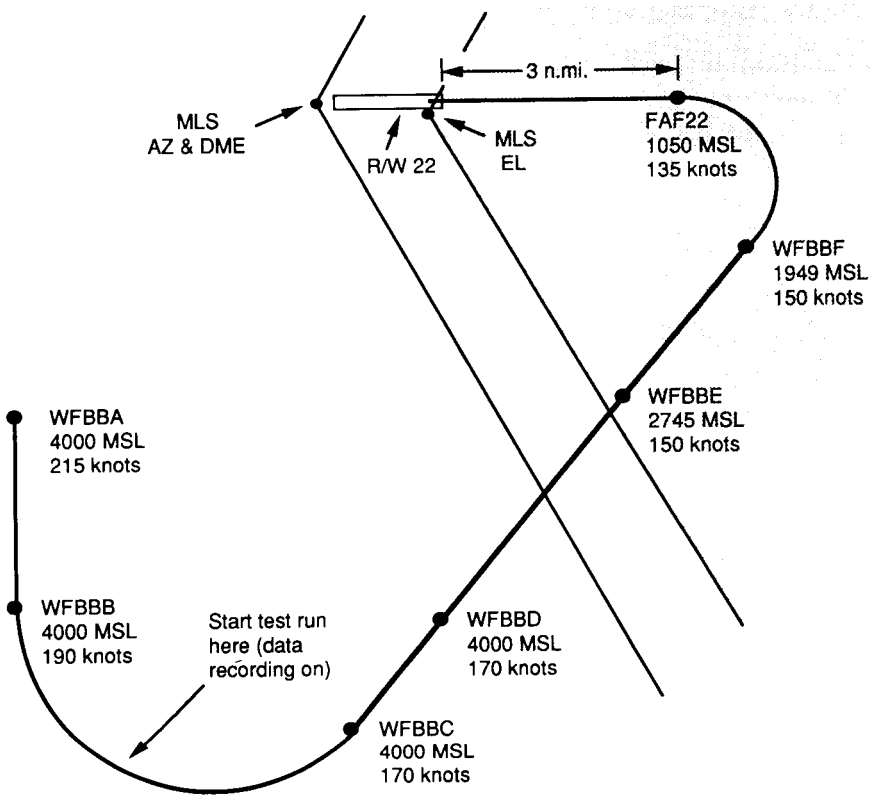

Figure 8. STAR WFB13 flight test path.

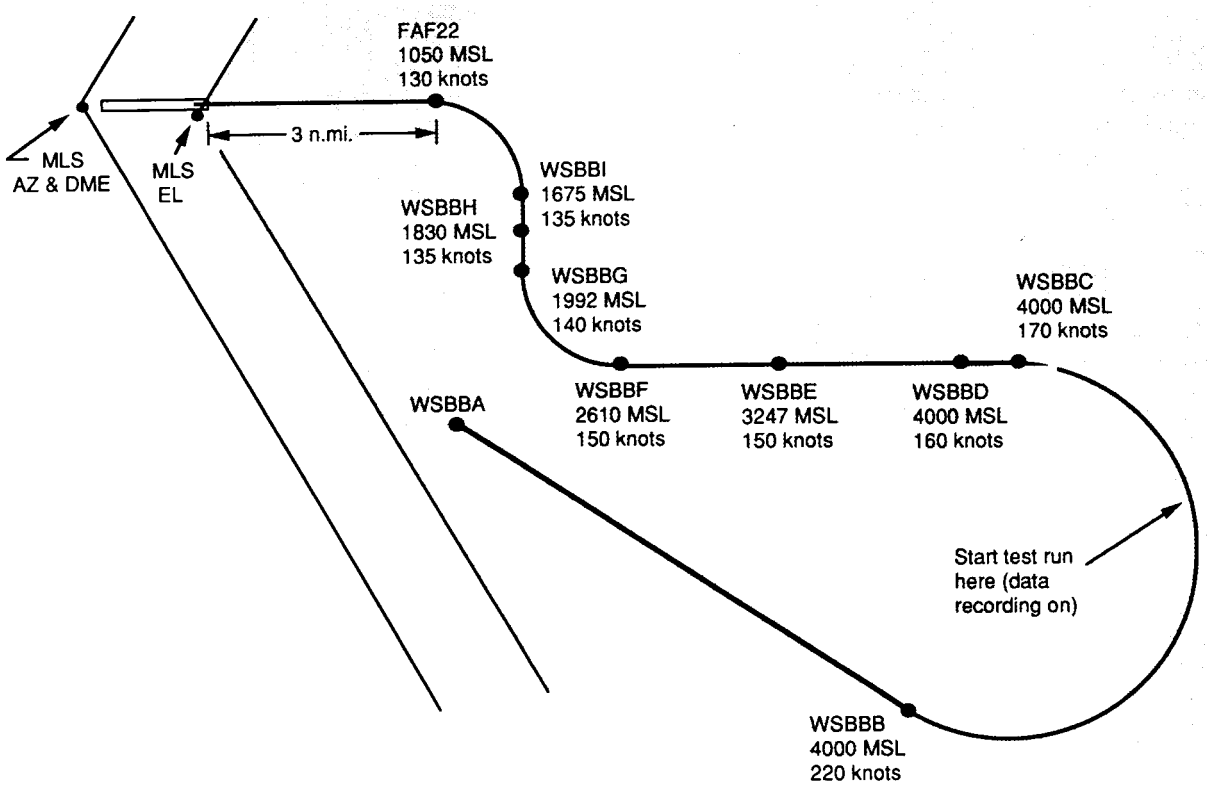

Figure 9. STAR WFSBB flight test path.

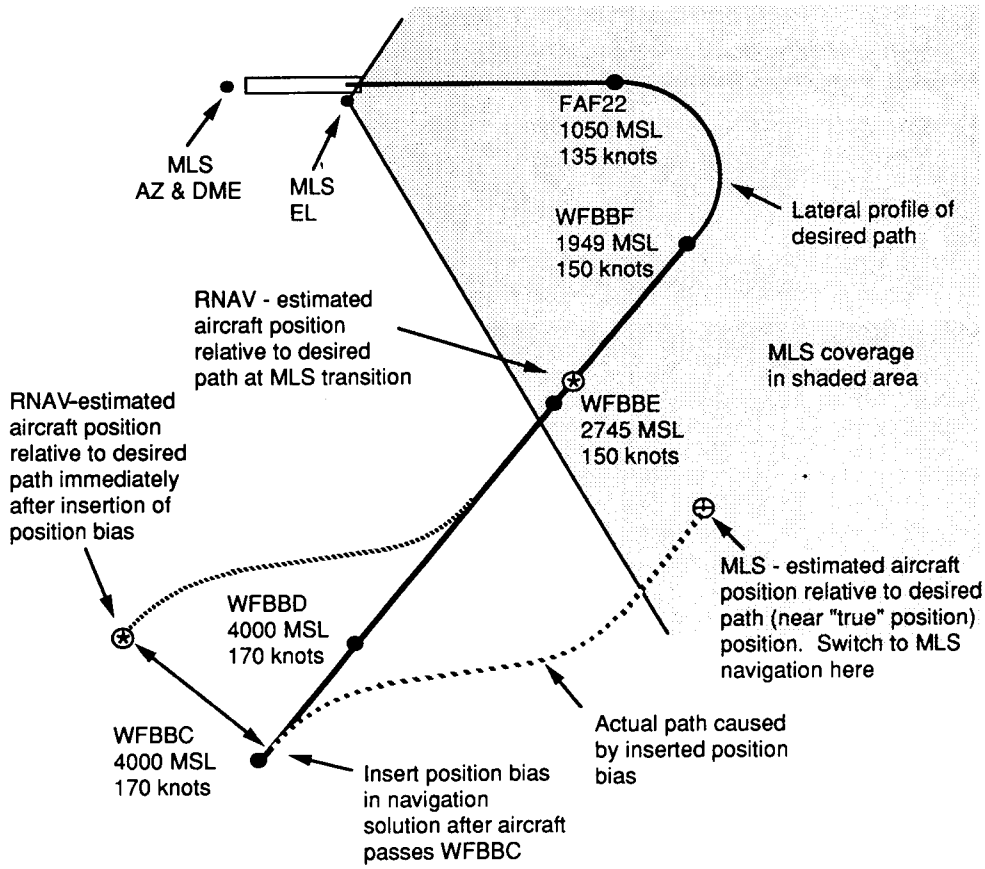

Figure 10. Illustration of aircraft ground track for inserted position bias.

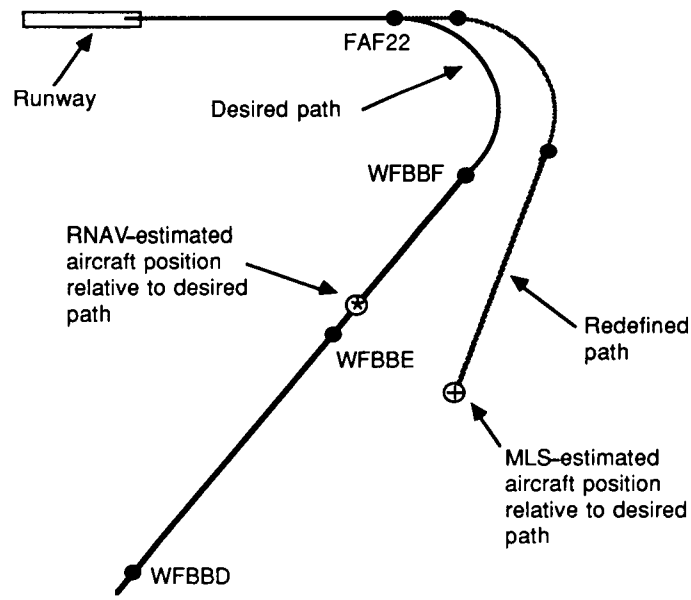

Figure 11. Typical map display on RNAV and redefined paths when MLS becomes valid.

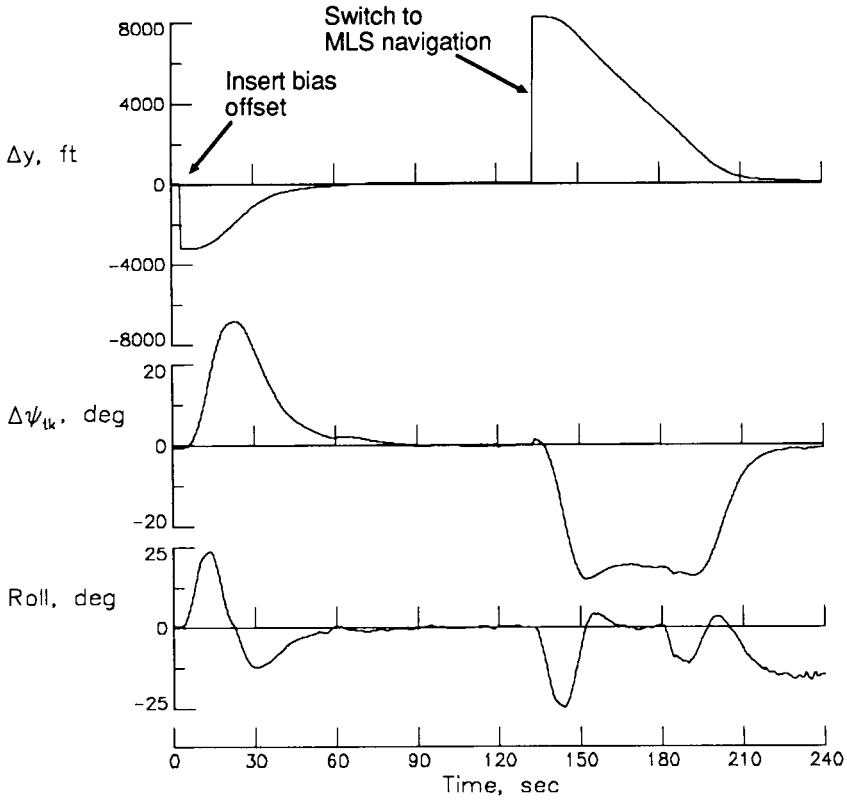

(a) Lateral response.

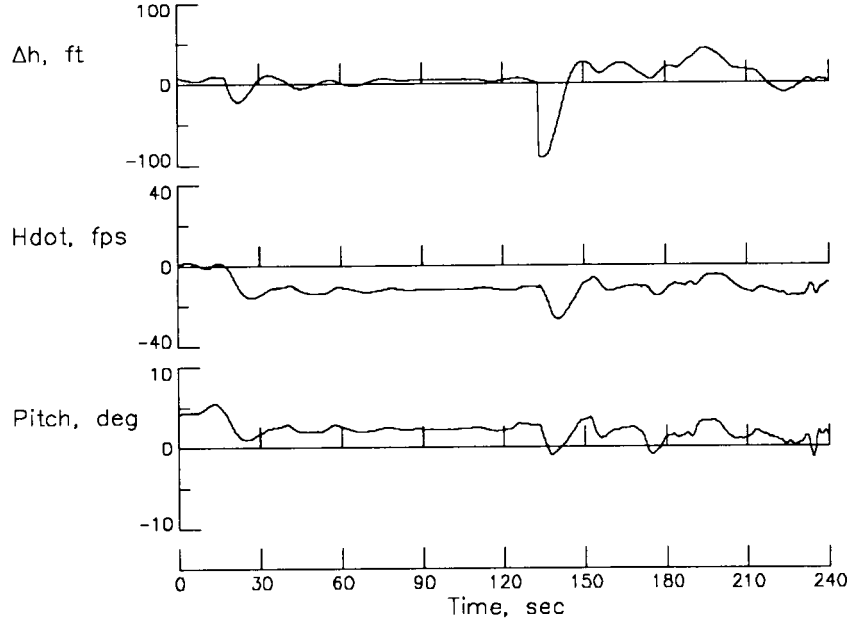

(b) Vertical response.

Figure 12. Time histories of selected parameters for test run 2.

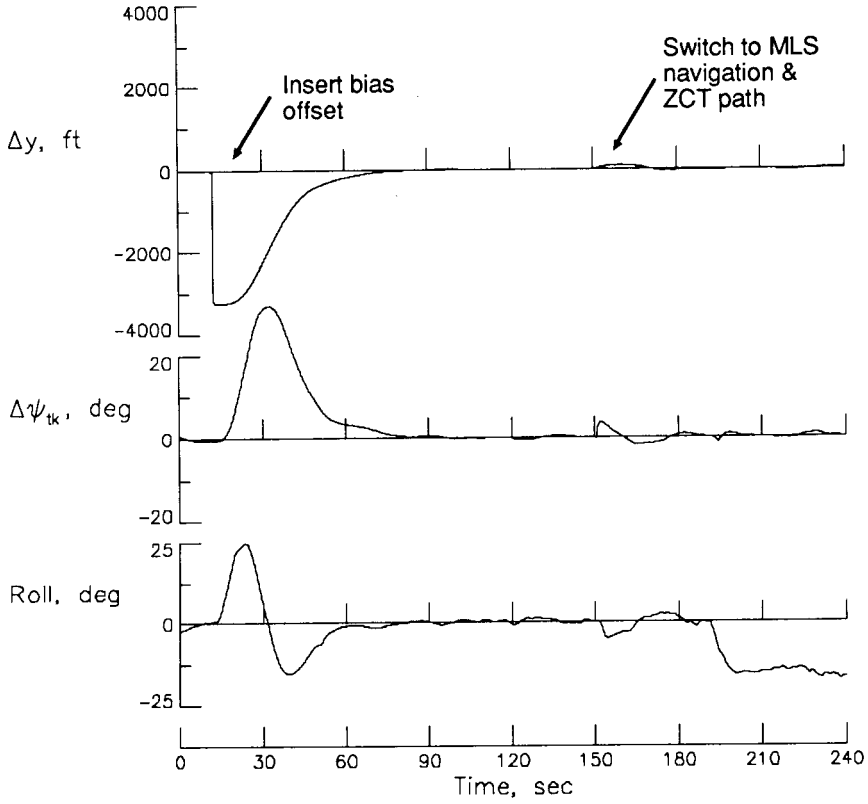

(a) Lateral response.

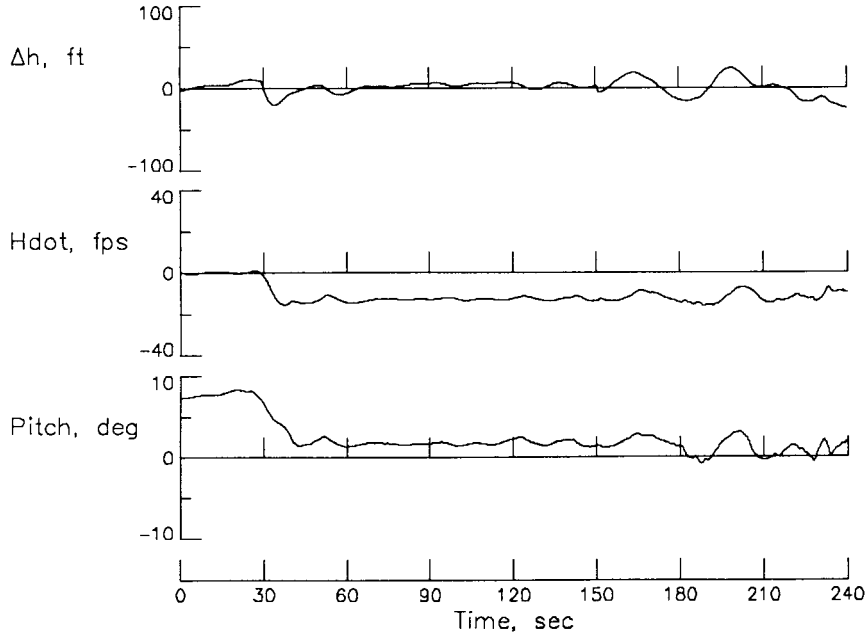

(b) Vertical response.

Figure 13. Time histories of selected parameters for test run 3 (ZCT algorithm).

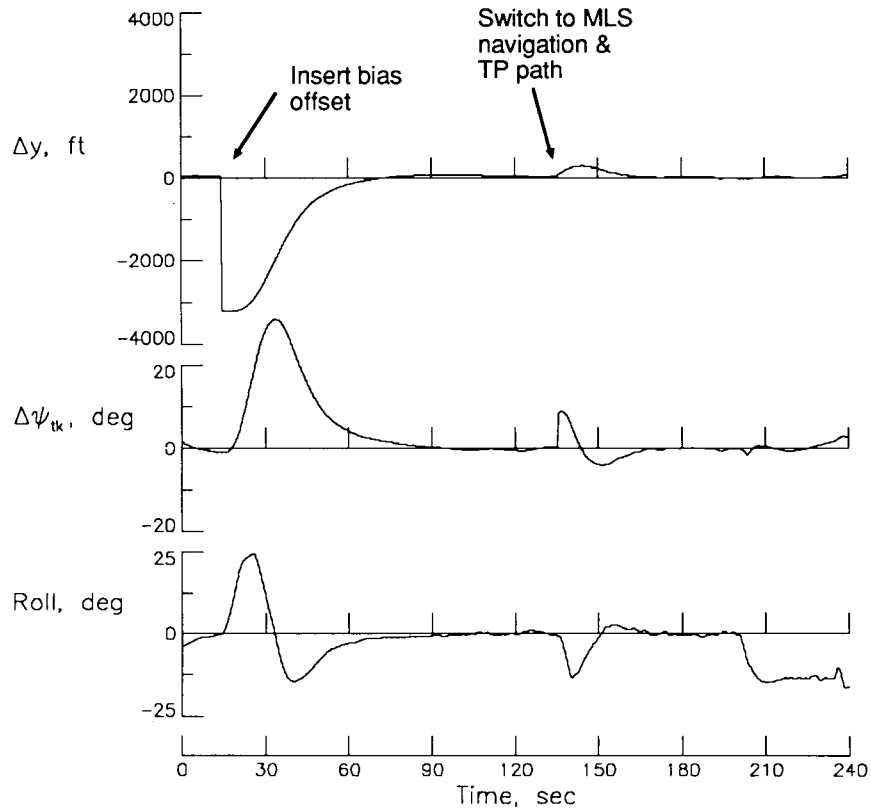

(a) Lateral response.

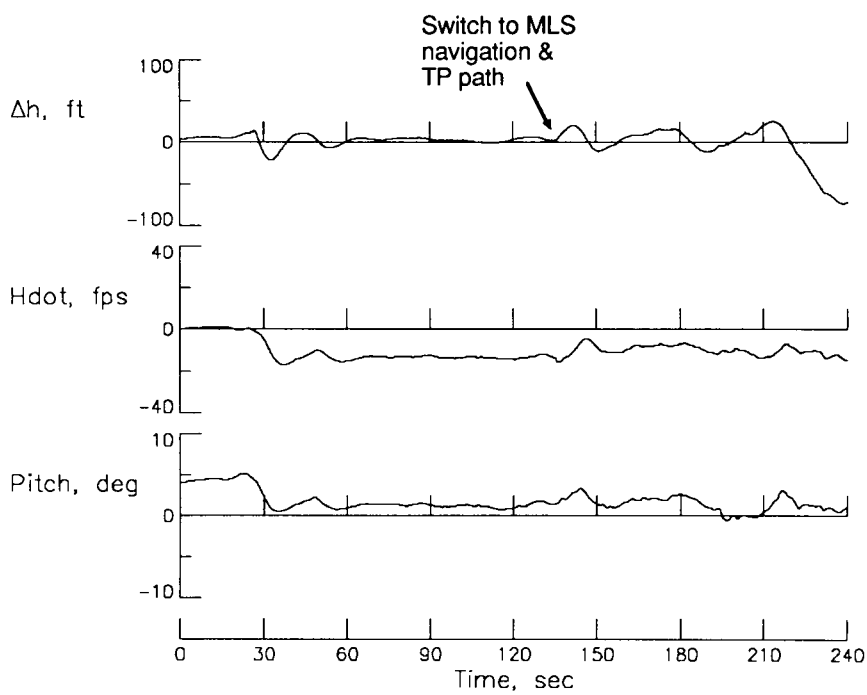

(b) Vertical response.

Figure 14. Time histories of selected parameters for test run 6 (TP algorithm).

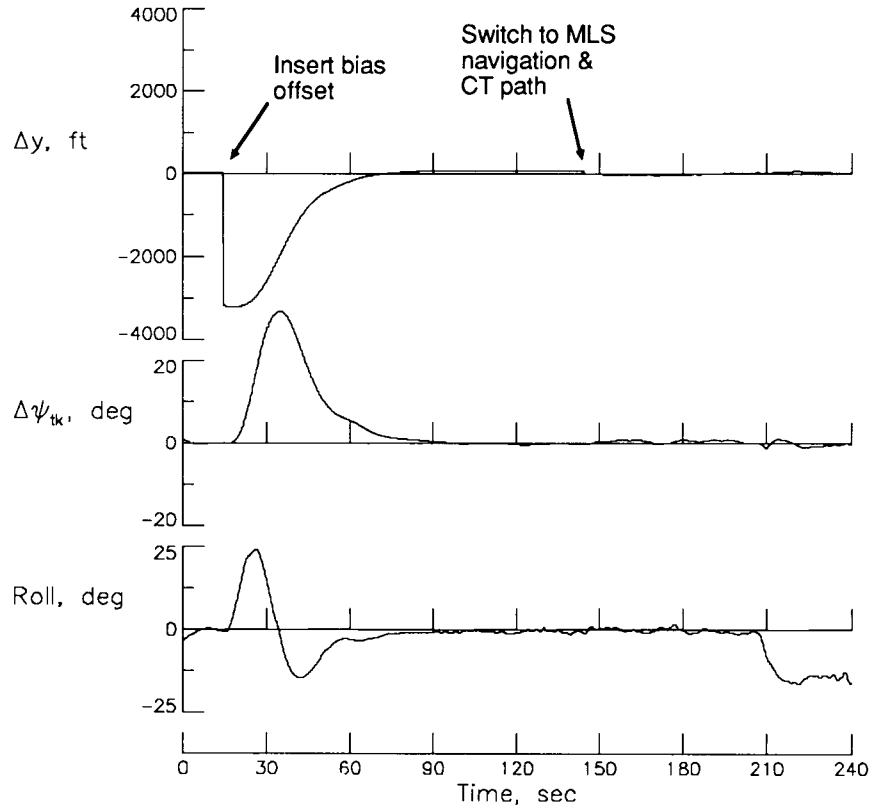

(a) Lateral response.

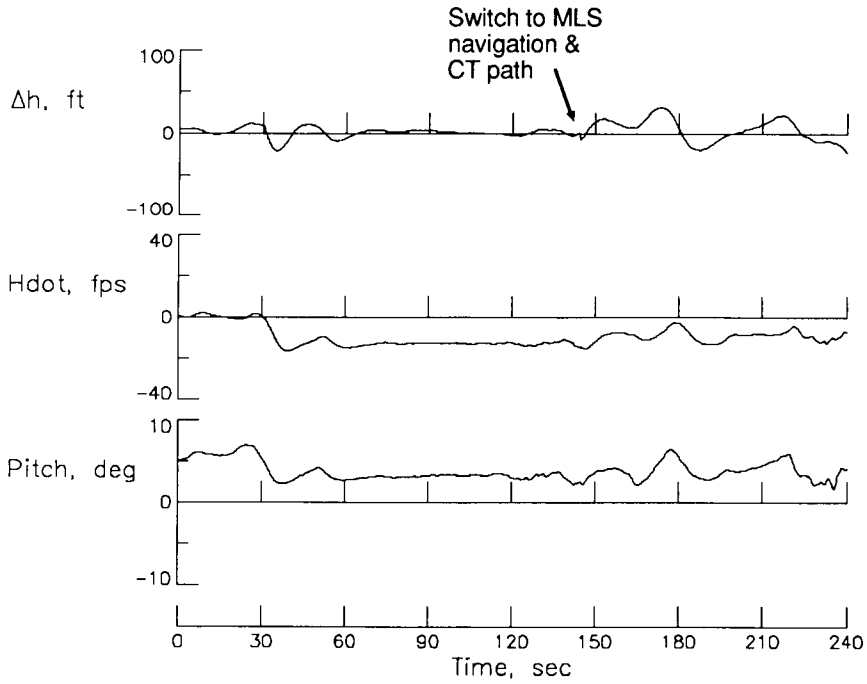

(b) Vertical response.

Figure 15. Time histories of selected parameters for test run 7 (CT algorithm).

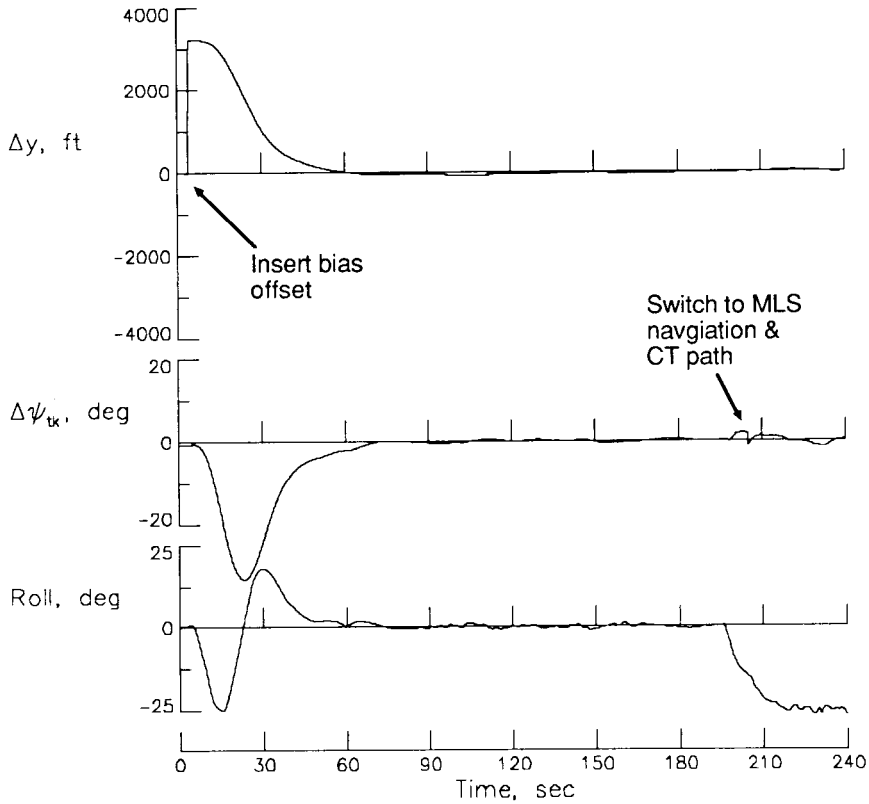

(a) Lateral response.

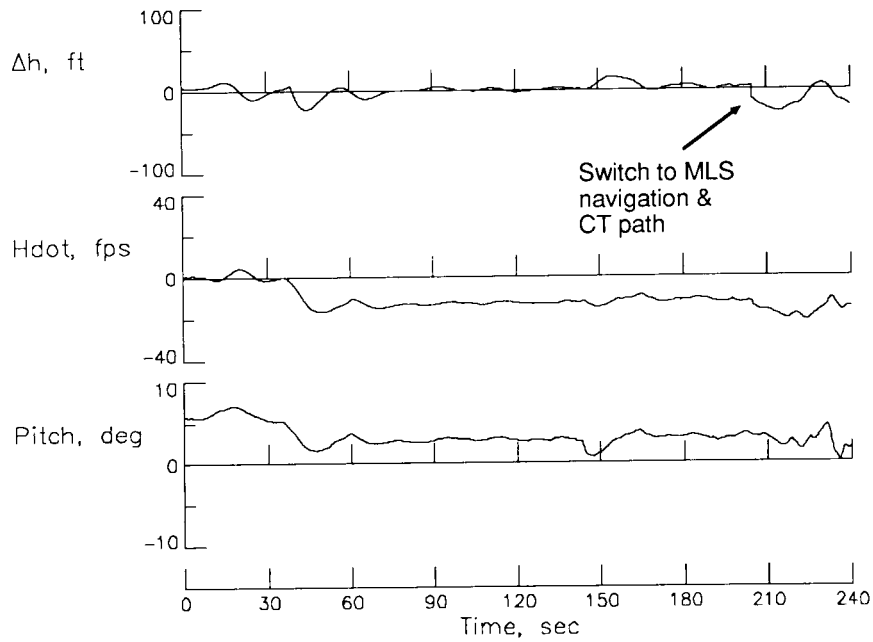

(b) Vertical response.

Figure 16. Time histories of selected parameters for test run 8 (CT algorithm in turn).

NASA
National Aeronautics and Space Administration

Report Documentation Page

1. Report No.	2. Government Accession No.	3. Recipient's Catalog No.
NASA TM-4089		

4. Title and Subtitle	5. Report Date
Flight Tests of Three-Dimensional Path-Redefinition Algorithms for Transition From Radio Navigation to Microwave Landing System Navigation When Flying an Aircraft on Autopilot	January 1989
	6. Performing Organization Code
7. Author(s)	8. Performing Organization Report No.
Richard M. Hueschen	L-16458
9. Performing Organization Name and Address	10. Work Unit No.
NASA Langley Research Center Hampton, VA 23665-5225	505-66-41-04
	11. Contract or Grant No.
12. Sponsoring Agency Name and Address	13. Type of Report and Period Covered
National Aeronautics and Space Administration Washington, DC 20546-0001	Technical Memorandum
	14. Sponsoring Agency Code

15. Supplementary Notes

16. Abstract

Three algorithms were developed in nonlinear aircraft simulations in an earlier effort to reduce autopilot-induced aircraft maneuvers at the transition to the Microwave Landing System (MLS) from radio navigation (RNAV). These maneuvers occur because of the large difference that can occur between the RNAV and MLS aircraft-position estimates. This report describes the algorithms and presents the results of flight tests that were conducted to validate the performance of the algorithms. Results are discussed and tabulated for two test runs where path-redefinition algorithms were not used and for nine test runs where they were used. Plots of flight test data are presented for five selected test runs. The results showed that all algorithms significantly reduced or eliminated the autopilot-induced aircraft maneuvering at the transition to the MLS.

17. Key Words (Suggested by Authors(s))	18. Distribution Statement
Navigation Guidance Three-dimensional flight and path definition Microwave Landing System (MLS)	Unclassified—Unlimited Subject Category 08

19. Security Classif.(of this report)	20. Security Classif.(of this page)	21. No. of Pages	22. Price
Unclassified	Unclassified	21	A03

NASA FORM 1626 OCT 86

NASA-Langley, 1989

For sale by the National Technical Information Service, Springfield, Virginia 22161-2171